



ELSEVIER

Nuclear Physics A 600 (1996) 236–250

NUCLEAR
PHYSICS A

Second order phase transitions: from infinite to finite systems

P. Finocchiaro^a, M. Belkacem^a, T. Kubo^{a,1}, V. Latora^{a,b}, A. Bonasera^a

^a INFN - Laboratorio Nazionale del Sud, Viale Andrea Doria (ang. Via S. Sofia), 95123 Catania, Italy

^b Dipartimento di Fisica, Università di Catania, 57, Corso Italia, 95129 Catania, Italy

Received 31 August 1995; revised 20 December 1995

Abstract

We investigate the Equation of State (EOS) of classical systems having 300 and 512 particles confined in a box with periodic boundary conditions. We show that such a system, independently on the number of particles investigated, has a critical density of about 1/3 the ground state density and a critical temperature of about 2.5 MeV. The mass distribution at the critical point exhibits a power law with $\tau = 2.23$. Making use of the grand partition function of Fisher's droplet model, we obtain an analytical EOS around the critical point in good agreement with the one extracted from the numerical simulations.

PACS: : 25.70.-z, 25.75.+r, 64.30.+t, 64.70.-p

1. Introduction

Recently, several experiments in proton–nucleus and nucleus–nucleus reactions have revealed the creation of fragment size distributions exhibiting power laws, expected according to the droplet model of Fisher, for fragment formation near the critical point of a liquid–gas phase transition [1]. This observation raised the question whether critical phenomena, which strictly speaking can only occur in the thermodynamic limit, can be explored within the context of heavy-ion collisions, where only a few hundreds of nucleons are involved [2].

In previous works [3], by studying the expansion of a classical finite system within the framework of Classical Molecular Dynamics (CMD), evidence has been found for

¹ Present address: Universität Tübingen, Institut für Theoretische Physik, D-71076 Tübingen, Germany.

the occurrence of a critical behaviour of our system revealed through a study of fragment size distributions, scaled factorial moments and moments of size distributions. Such a critical behaviour is connected to a liquid–gas phase transition by the use of Fisher’s droplet model [4] and Campi analysis [5]. In the present work, using the same two-body interaction [6], we calculate by means of the virial theorem [2,8], the equation of state of a classical system confined in a cubic box with constant density and periodic boundary conditions. This equation of state has a critical temperature of about 2.5 MeV and a critical density of about one third the ground state density. Trajectories in the (ρ, T) plane of expanding finite systems indeed go through this critical point [3]. It is also shown that at the critical point, the fragment size distribution exhibits a power law with $\tau = 2.23$, consistent with the droplet model of Fisher [3,4], and scaling laws of critical exponents for a liquid–gas phase transition.

We calculate in Section 2, within the framework of CMD [3,6], the equation of state of the system in a cubic box with cyclic boundary conditions. Section 3 contains the study of fragment size distributions at the critical point and around it. In Section 4, we study the critical behaviour of the moments of size distributions using the grand partition function of the Fisher’s droplet model and extract the equation of state of this model in the vicinity of the critical point, which is found in good agreement with the one calculated for the infinite system. Finally, we give our summary and conclusions in Section 5.

2. Equation of state

In the following, making use of the virial theorem [2,8], we study the equation of state of classical systems with 300 particles (150 protons + 150 neutrons) and 512 particles (256 protons + 256 neutrons) confined in a cubic box with periodic boundary conditions. The particles of the system move under the influence of a two-body potential V given by [6]:

$$\begin{aligned} V_{np}(r) &= V_r [\exp(-\mu_r r)/r - \exp(-\mu_r r_c)/r_c] \\ &\quad - V_a [\exp(-\mu_a r)/r - \exp(-\mu_a r_a)/r_a], \\ V_{nn}(r) &= V_{pp}(r) = V_0 [\exp(-\mu_0 r)/r - \exp(-\mu_0 r_c)/r_c], \end{aligned} \quad (1)$$

$r_c = 5.4$ fm is a cutoff radius. V_{np} is the potential acting between a neutron and a proton while V_{nn} is the potential acting between two identical nucleons. The first potential is attractive at large r and repulsive at small r , while the latter is purely repulsive so no bound state of identical nucleons can exist. The various parameters entering Eq. (1) are defined with their respective values in Ref. [6]. The classical Hamilton’s equations of motion are solved using the Taylor method at the order $O[(\delta t)^2]$ where δt is the integration time step [9]. Energy and momentum are well conserved because we use a very small time step δt varying in time according to the maximum acceleration of the particles.

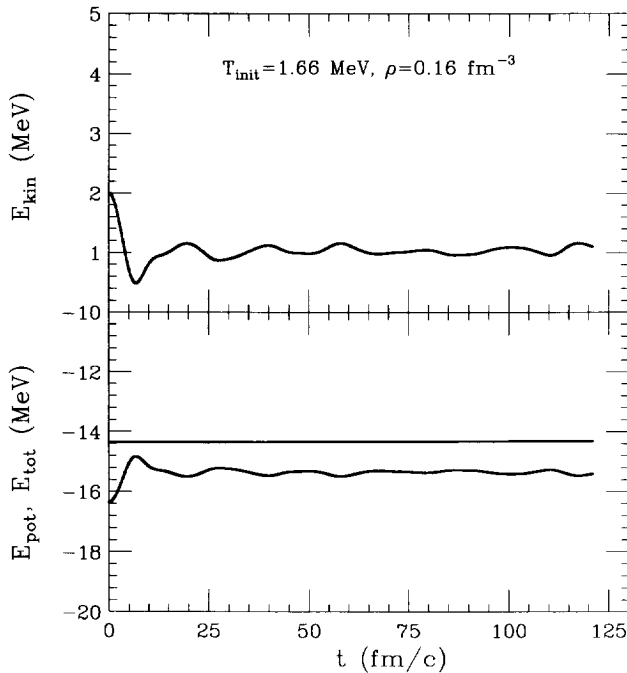


Fig. 1. Kinetic energy (upper part), potential energy (lower part, lower line) and total energy (lower part, upper line) are plotted versus time for the system with 512 particles using the second method for thermalization (see text). The density is fixed at $\rho = 0.16 \text{ fm}^{-3}$ and the system is initialized at a temperature $T = 1.66 \text{ MeV}$.

Two different methods were used for initialization and thermalization of the system. In the first one, the particles are initially distributed randomly in a cubic box with a small size (the initial density is about 0.32 fm^{-3}) and they are given the same velocity modulus which is quite large. The system is then cooled down to a predefined average kinetic energy by rescaling the velocities at each time iteration by a coefficient close to unity. After the density is decreased slowly to the desired density (at each time iteration the size of the box is slowly increased). During the cooling process, the system also thermalizes. Nevertheless, after the desired density and temperature have been reached, we let it evolve for additional time to allow a complete thermalization. In the second method, the particles are initially distributed on a cubic lattice such as the nearest neighbors of a proton are all neutrons and vice versa, and the system is excited at an initial temperature giving to its particles a maxwellian velocity distribution by means of a Metropolis sampling [9]. The system then evolves according to Hamilton's equations of motion and reaches equilibrium after few thousands of iterations. With the first method, the system reaches equilibrium faster than with the second one.

In Fig. 1 we have plotted the time evolution of the kinetic energy (upper part), the potential energy (lower part, lower line) and total energy (lower part, upper line) computed using the second method for thermalization for the system with 512 particles. The density of the system is fixed at $\rho = 0.16 \text{ fm}^{-3}$ and the initial temperature is set at $T = 1.66 \text{ MeV}$. We see that the total energy is well conserved during all the time

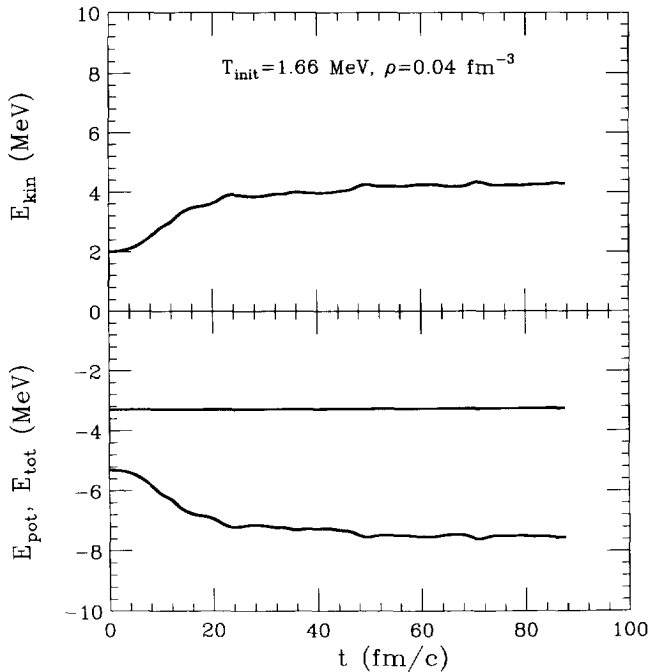


Fig. 2. Same as Fig. 1 but the density of the system is fixed at $\rho = 0.04 \text{ fm}^{-3}$.

evolution (2.5% in 100 fm/c). In this case the system thermalizes very quickly in the first 20 fm/c, then the kinetic energy stabilizes around 1.0 MeV ($T = 0.7 \text{ MeV}$) with small fluctuations due to the interplay between kinetic and potential energy. In Fig. 2 we plot the same quantities at a density of 0.04 fm^{-3} and the same initial temperature $T = 1.66 \text{ MeV}$. In this case we see that the thermalization process takes a longer time and the kinetic energy stabilizes around 4 MeV.

In the following, the calculations are done using the first method of initialization and thermalization for the system with 300 particles (150 protons + 150 neutrons). The results obtained with the second method for the system with 512 particles (256 protons + 256 neutrons) are totally consistent with those presented here and give the same equation of state with the same critical point.

After the system has thermalized, we calculate the equation of state of our system by means of the virial theorem. The pressure of a system of classical particles interacting through two-body forces is given by [2,7,8]

$$\begin{aligned}
 P(\rho, T) &= \rho T + \frac{1}{6V} \int d\mathbf{r}_1 d\mathbf{r}_2 |\mathbf{r}_1 - \mathbf{r}_2| F_{12}(\mathbf{r}_1 - \mathbf{r}_2) n_2(\mathbf{r}_1, \mathbf{r}_2) \\
 &= \frac{2}{3V} \left\langle \sum_i E_i \right\rangle + \frac{1}{3V} \left\langle \sum_{i < j} |\mathbf{r}_i - \mathbf{r}_j| \cdot F_{ij}(\mathbf{r}_i - \mathbf{r}_j) \right\rangle, \tag{2}
 \end{aligned}$$

where V is the volume of the box, $\rho = A/V$ the density, $F_{ij} = -dV_{ij}/dr$ is the force acting between particles i and j , and $n_2(\mathbf{r}_1, \mathbf{r}_2)$ is the pair distribution function. E_i is the

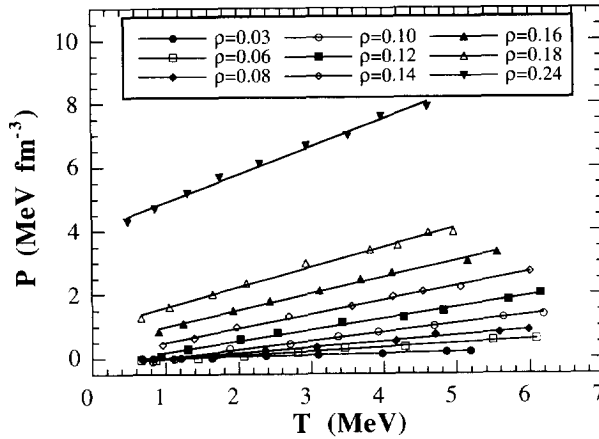


Fig. 3. The pressure P of the system, calculated using the virial theorem, is plotted versus temperature T for several values of the density ranging from 0.03 to 0.24 fm^{-3} . The points indicate the results of the numerical simulations, and the solid lines the linear fits. The temperatures considered are the ones at equilibrium.

kinetic energy of particle i , and the brackets $\langle \dots \rangle$ denote the time average. In the above equation, the Boltzmann constant k is set equal to 1. To calculate the pressure, we let the system evolve after the thermalization for additional time and take the average over this time evolution. The density of the system is fixed, while the temperature is given in the equilibrium phase by 2/3 of the kinetic energy.

In Fig. 3 we have plotted the pressure P versus the final temperature of the system T for several values of the density ρ ranging from 0.02 to 0.24 fm^{-3} . We see from the figure that for all the values of the density considered, the pressure P shows a linear behaviour versus temperature,

$$P(\rho, T) = a(\rho)T + b(\rho). \quad (3)$$

Note that the temperatures considered here are that of the thermalized system (at equilibrium). The values of the fitting parameters $a(\rho)$ and $b(\rho)$ are plotted in the upper and lower parts of Fig. 4, respectively, versus the density ρ (solid dots). At this point, to determine the equation of state, we fitted the parameters $a(\rho)$ and $b(\rho)$ with polynomials in ρ with the minimum number of fitting parameters and the following constraints: i) all the isotherms have a zero pressure at zero density $P(\rho = 0, T) = 0$, which means $a(0) = b(0) = 0$; ii) the isotherm $T = 0$ MeV has a zero slope at zero density $\partial P/\partial \rho|_{T=0, \rho=0} = 0$, which means $\partial b/\partial \rho|_{\rho=0} = 0$. The resulting polynomial fits give:

$$\begin{aligned} P(\rho, T) &= (a_1\rho + a_2\rho^2)T + b_2\rho^2 + b_3\rho^3 \\ &= (0.96\rho + 7.13\rho^2)T - 87.0\rho^2 + 646.0\rho^3. \end{aligned} \quad (4)$$

The fits to $a(\rho)$ and $b(\rho)$ are shown by solid lines in Fig. 4. Note that the parameter a_1 is almost equal to 1 which means that our equation of state is in agreement with that of a classical gas at high temperature and low density $\rho \rightarrow 0, T \rightarrow \infty \Rightarrow P \approx \rho T$. Turning off the two-body potential, the law of ideal gases is respected within less than

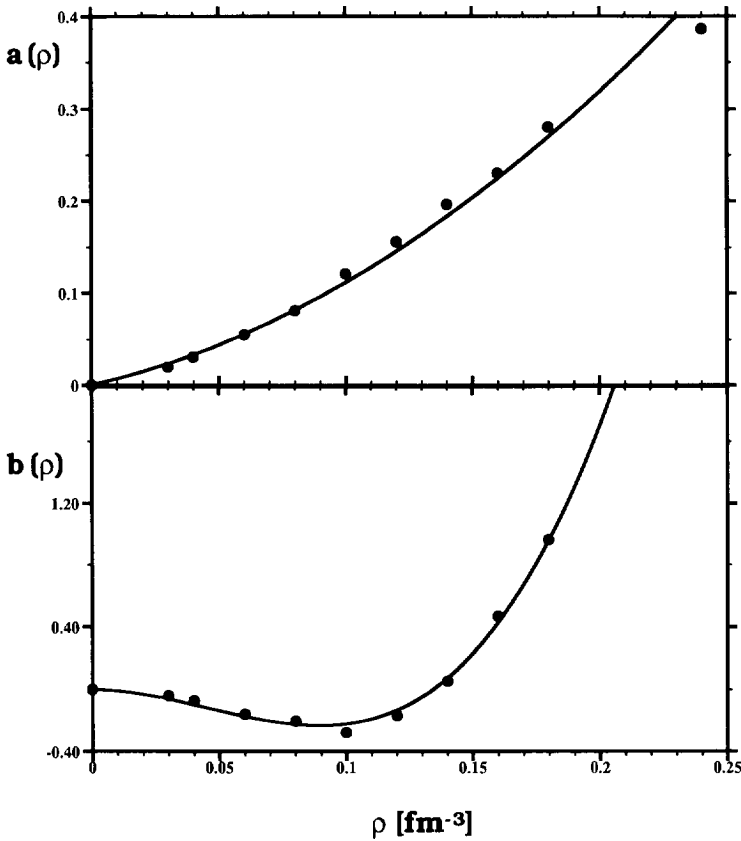


Fig. 4. The values of the fitting parameters $a(\rho)$ (upper part) and $b(\rho)$ (lower part) are plotted versus density ρ (solid points). The solid lines show the polynomial fits to these values (see text).

1%. We have plotted in Fig. 5 the pressure P , Eq. (4), versus density for several values of the temperature T . The dashed line in the figure delimits the isothermal spinodal region given by

$$\left. \frac{\partial P}{\partial \rho} \right|_T < 0. \tag{5}$$

The obtained equation of state Eq. (4) has a critical point

$$T_c = 2.53 \text{ MeV}; \quad \rho_c = 0.04 \text{ fm}^{-3}; \quad P_c = 0.029 \text{ MeV} \cdot \text{fm}^{-3}. \tag{6}$$

Note that the ratio $P_c/T_c\rho_c = 0.32$ is in good agreement with the experimental values for real gases which give for example 0.287 for CO_2 , 0.290 for Xe and 0.305 for ${}^4\text{He}$. We have also plotted in Fig. 6 the isothermal spinodal line (Eq. (5)) in the plane $(\rho/\rho_c, T/T_c)$ together with the experimental values for eight different substances in the gas-liquid coexistence region [10]. The critical data for all these substances are quite varied (see Ref. [10]), but the reduced data points fall on a universal curve. The right branch refers to the liquid phase, and the left branch to the gas phase, and both come together

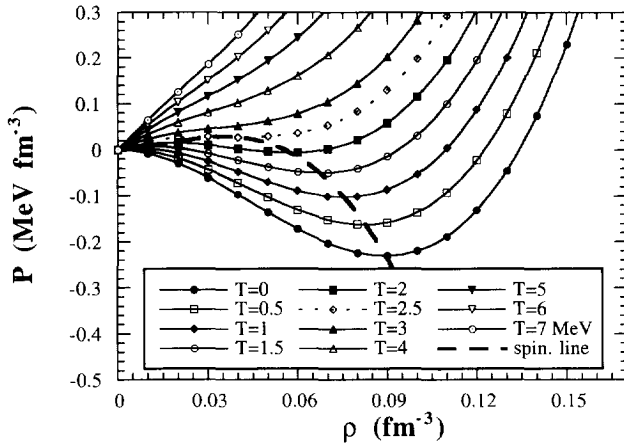


Fig. 5. The pressure P , calculated using the obtained equation of state Eq. (4), is plotted versus density ρ for several values of temperature T . The dashed line indicates the isothermal spinodal line of the EOS. The critical isotherm is indicated by the small-dashes line.

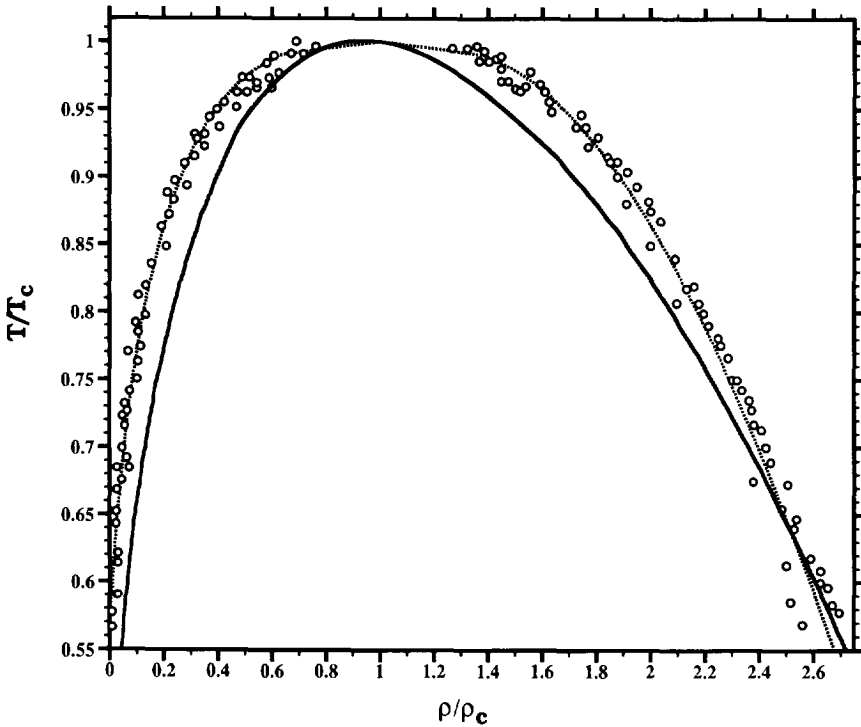


Fig. 6. Reduced temperature versus reduced density in the gas–liquid coexistence region for our system (solid line) and for eight different substances: Ne, Ar, Kr, Xe, N_2 , O_2 , CO and CH_4 (open circles). The dashed line shows Guggenheim's fit.

at the critical point. Our coexistence curve falls also, with some small differences, on the same universal curve. The dashed line shows Guggenheim's fit [10].

As already stated, using the second method of initialization and thermalization for the system with 512 particles we obtained the same equation of state Eq. (4) with less than 5% difference with the first method using a system with 300 particles. This allows us to conclude that the equation of state of our system does not depend on the number of particles we have used in the box, and on the way how the system has reached equilibrium.

3. Mass distributions

In this section, our aim is to generate the mass distributions at the critical point and around it to see whether one gets a power law at the critical point as predicted by the droplet model of Fisher [4], and as observed in CMD for an expanding classical system [3]. To do so, we generate many events near the critical temperature, and at the critical density $\rho_c = 0.04 \text{ fm}^{-3}$. Unfortunately, our algorithm of cluster recognition which is of the percolation-type, is not able to identify the fragments inside the box, even at such small density [11]. In this algorithm, the fragments are defined as follows. It is possible to go from any particle i to another particle j belonging to the same fragment by successive interparticle jumps of a prescribed distance d or less (in these calculations, d is set equal to the range of the two-body potentials $d = r_c = 5.4 \text{ fm}$), but any path to a particle k belonging to another fragment contains one or more jumps of distance greater than d . This kind of cluster recognition algorithms is not indicated for identifying fragments confined in a box because the results are very dependent on the choice of the distance d . However, for expanding systems with fragments flying away from each other, these algorithms work well, particularly by following the fragments in time. To overcome this inherent problem, after the system has thermalized and the fragments are formed inside the box, we take off the box and let the system expand and the fragments fly away for enough time to allow a good identification of the fragments.

Because this procedure is very CPU-time consuming, we have generated only 100 events of the system with 216 particles (108 protons + 108 neutrons) at each temperature and calculated the mass distributions from these events. The results of these calculations are drawn in Fig. 7, where we have plotted the mass distributions obtained from the expansion of system prepared at the critical density $\rho_c = 0.04 \text{ fm}^{-3}$ and temperatures (at thermalization) $T = 2.0 \text{ MeV}$, $T_c = 2.54 \text{ MeV}$ and $T = 3.92 \text{ MeV}$. At the critical temperature, apart for large masses where one observes large fluctuations due to the limited number of events generated, one observes a power law, consistent with the droplet model of Fisher, with a power $\tau = -2.23$, the same as the one found for the expanding finite system passing during its expansion through the critical point. Below the critical temperature, one observes a mass distribution with a "U" shape characteristic to undercritical events where one sees some remaining of the initial system, and above the critical temperature one observes a rapidly decreasing mass distribution

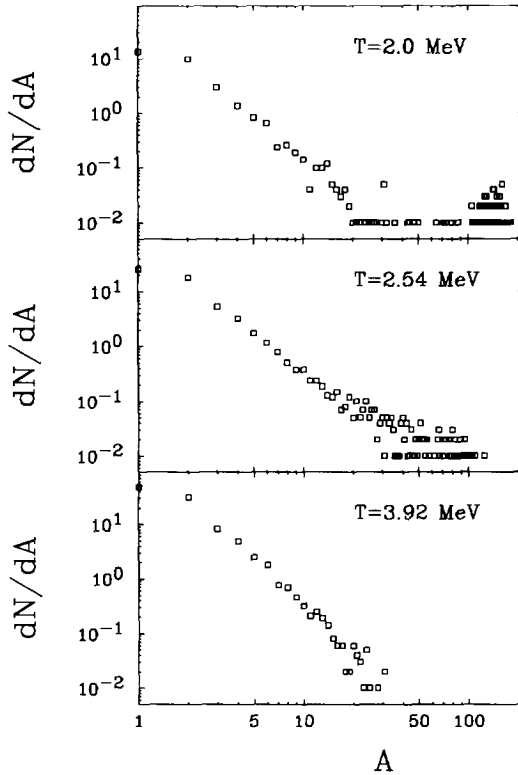


Fig. 7. Mass distributions obtained for the fragmentation of the system with 216 particles with three different temperatures (at equilibrium) $T = 2.0$ MeV (upper part), $T_c = 2.54$ MeV (central part) and $T = 3.92$ MeV (lower part).

with an exponential shape characteristic to highly excited systems going to complete vaporization.

4. Fisher's droplet model and the equation of state

Fisher's droplet model has successfully been applied to describe the fragmentation of excited classical systems which expand and, depending on the excitation energy show different dynamical evolutions, from evaporation like processes (small excitation energy) to multifragmentation and complete vaporization of the system (for large excitation energies) [3].

In the following, using the grand partition function Fisher has derived for a large system of individual particles in which clusters of two, three and more particles are bound together by the attractive forces, and in mutual statistical equilibrium with the remaining parts of the system and the surrounding gas [12]. In this model, the grand partition function

$$\Xi(z, V, \beta) = \sum_{N=0}^{\infty} z^N Q_N(V, \beta), \tag{7}$$

where $z = e^{\beta\mu}$ is the fugacity, $\beta = 1/T$ and $Q_N(V, \beta)$ is the canonical partition function, is given by

$$\ln \Xi(\mu, V, T) = \sum_{A=1}^{\infty} Y(A), \tag{8}$$

where $Y(A)$ is the probability to find a cluster of size A in the system (cluster size distribution) and is given by [12]

$$Y(A) = Y_0 A^{-\tau} \exp \left[\beta\mu A - \beta b A^{2/3} \right] = Y_0 A^{-\tau} B A^{2/3} S^A, \tag{9}$$

where $\mu = \mu_g - \mu_l$ is the difference between the chemical potentials of the gas and liquid phases. b denotes the surface contribution to the Gibbs free energy and is proportional to the surface tension. The term $A^{-\tau}$ has been introduced by Fisher to take into account the fact that the droplet surface closes on itself. The parameter τ is related to some critical exponents through scaling laws of critical phenomena and thus has a constant value in the range $2 < \tau < 2.5$ [4,12]. Knowing the grand partition function, the equation of state of the system is given by

$$P = \frac{T}{V} \ln \Xi(\mu, V, T) = \frac{T}{V} \sum_{A=1}^{\infty} Y(A),$$

$$\langle N \rangle = z \frac{\partial}{\partial z} \ln \Xi(\mu, V, T) = \sum_{A=1}^{\infty} A Y(A) \tag{10}$$

and the isothermal compressibility is given by,

$$\chi_T = \frac{VT}{\langle N \rangle^2} \frac{\partial^2}{\partial \mu^2} \ln \Xi(\mu, V, T) = \frac{V}{T \langle N \rangle^2} \sum_{A=1}^{\infty} A^2 Y(A). \tag{11}$$

Defining the moments of the cluster size distributions $Y(A)$ by

$$M_k = \sum_{A=1}^{\infty} A^k Y(A) \tag{12}$$

gives for the previous quantities

$$P = \frac{T}{V} M_0,$$

$$\langle N \rangle = M_1 \implies \rho = \frac{\langle N \rangle}{V} = \frac{M_1}{V} \tag{13}$$

and

$$\chi_T = \frac{1}{VT\rho^2} M_2. \tag{14}$$

From Eqs. (13), one obtains the equation of state in terms of the zeroth and first moments of the cluster size distribution

$$P = T\rho M_0/M_1. \tag{15}$$

More generally, the moments of the cluster size distributions are related to Fisher’s grand partition function by:

$$M_k = \left(T \frac{\partial}{\partial \mu} \right)^k \ln \Xi(\mu, V, T). \tag{16}$$

The equation of state Eq. (15) is useless because of the complexity in estimating in a model independent way the cluster size distributions $Y(A)$ (Eq. (9)) and hence the moments M_k . However, an estimate of the moments in the vicinity of the critical point is possible by making a few approximations. In the formula for the cluster size distributions Eq. (9), for temperatures equal or larger than the critical temperature $T \geq T_c$, the surface term b vanishes because it is proportional to the surface tension which is equal to 0 for $T \geq T_c$ and the difference of chemical potentials μ is negative

$$Y(A) = Y_0 A^{-\tau} \exp(\beta\mu A), \quad T \geq T_c. \tag{17}$$

We can now use the well known formula by Robinson derived for the Bose–Einstein integral [13]:

$$\sum_{A=1}^{\infty} e^{-A\alpha} A^{-\sigma} = \Gamma(1 - \sigma) \alpha^{\sigma-1} + \sum_{n=0}^{\infty} \frac{(-1)^n}{n!} \zeta(\sigma - n) \alpha^n. \tag{18}$$

where $\alpha > 0$.

Using this formula, the moments of the cluster size distribution become for $T \geq T_c$:

$$M_k = Y_0 \left[\Gamma(1 + k - \tau) |\beta\mu|^{-(1+k-\tau)} + \sum_{n=0}^{\infty} \frac{(-1)^n}{n!} \zeta(\tau - k - n) |\beta\mu|^n \right]. \tag{19}$$

The second term in the rhs of the above equation is regular and hence, while the zeroth and first moments are always finite because τ is limited between 2 and 2.5, the higher moments diverge as

$$M_k \propto |\beta\mu|^{-(1+k-\tau)}. \tag{20}$$

By assuming $\mu = (T - T_c)^\nu$, one recovers the formula Campi has derived for the moments at the critical point [5]

$$M_k \propto |T - T_c|^{-\nu(1+k-\tau)}. \tag{21}$$

In the vicinity of the critical point, the difference of chemical potentials μ tends to zero and one can consider the lowest orders only in the expansion of the moments M_k in terms of powers of μ , Eq. (19), which gives for the pressure P and density ρ (assuming $\tau = 2.33$):

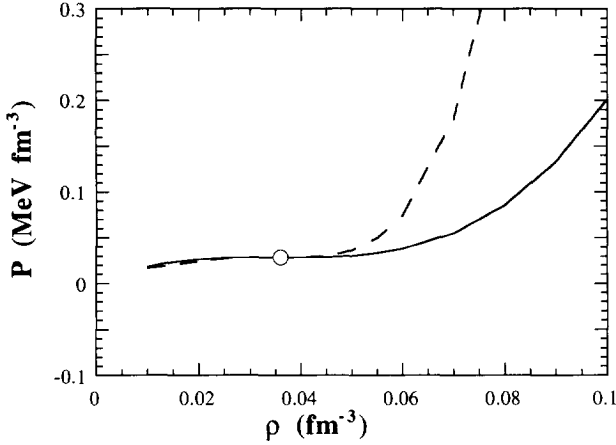


Fig. 8. Pressure versus density. The solid line shows the critical isotherm of the equation of state obtained in Section 2 by numerical simulations of a classical system, and the dashed line the critical isotherm of the analytical EOS obtained in Section 4 using Fisher's droplet model. The open circle indicates the critical point.

$$\begin{aligned}
 P &= q_0 T \left[3.072 |\beta \mu|^{4/3} + 1.417 - 3.631 |\beta \mu| + \dots \right], \\
 \rho &= q_0 \left[-4.086 |\beta \mu|^{1/3} + 3.631 + 0.966 |\beta \mu| + \dots \right],
 \end{aligned}
 \tag{22}$$

where $q_0 = Y_0/V$. At the critical point, $\mu = 0$ and one gets,

$$P_c = 1.417 q_0 T_c, \quad \rho_c = 3.631 q_0.
 \tag{23}$$

Subtracting Eqs. (22) and (23) gives,

$$\begin{aligned}
 P - P_c &= q_0 T \left[3.072 |\beta \mu|^{4/3} - 3.631 |\beta \mu| + \dots \right] + 1.417 q_0 (T - T_c), \\
 \rho - \rho_c &= q_0 \left[-4.086 |\beta \mu|^{1/3} + 0.966 |\beta \mu| + \dots \right].
 \end{aligned}
 \tag{24}$$

Combining the above equations and taking the lowest orders in terms of powers of μ , we get the following equation of state, valid in the vicinity of the critical point

$$P - P_c = 1.417 q_0 (T - T_c) + \frac{0.0532}{q_0^2} T (\rho - \rho_c)^3 + \frac{0.011}{q_0^3} T (\rho - \rho_c)^4.
 \tag{25}$$

Using the numerical values of the critical temperature, density and pressure, obtained in Section 2 for the system in a box with periodic boundary conditions (Eq. (6)), we have plotted in Fig. 8, the critical isotherm of the above equation of state in the vicinity of the critical point (dashed line). In the same figure, we have also plotted the critical isotherm of the equation of state obtained in Section 2, Eq. (4) (solid line). The critical point is indicated in the figure by the open circle. We see from the figure that the two curves go on each other in the vicinity of the critical point, while they start to deviate going away from the critical region.

From Eq. (16), we see that the isothermal compressibility χ_T is related to the second moment M_2 . At the critical point, the isothermal compressibility becomes infinite, and so

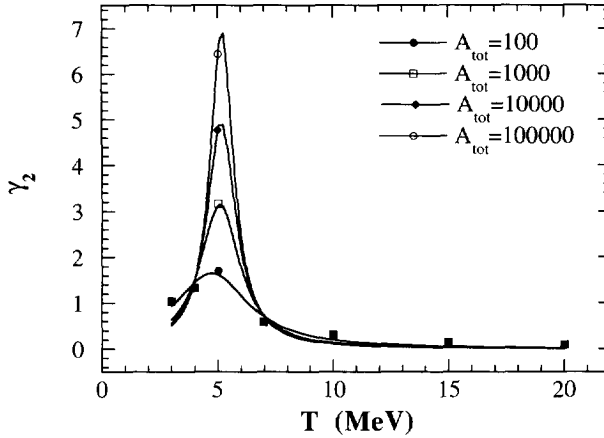


Fig. 9. The reduced variance γ_2 is plotted versus the initial temperature for the expansion of a finite system (see text) for several values of the size of the system A_{tot} .

the second moment diverges, which means that the fluctuations of cluster sizes expressed by the second moment M_2 become very large at the critical point. Defining the relative variance γ_2 , introduced by Campi to have more insight in the shape of the cluster size distributions and to indicate the critical behaviour [5],

$$\gamma_2 = \frac{M_2 M_0}{M_1^2}, \quad (26)$$

one expects that this quantity diverges at the critical point. Of course, if one considers a finite system, the moments remain finite, and instead of a divergence, the relative variance γ_2 shows a peak around the critical point. To study finite size effects on the relative variance γ_2 , we calculate the moments of cluster size distributions $Y(A)$ using for the parameters Y_0 , τ , B and S appearing in Eq. (9) the values obtained by fitting the fragment mass distributions obtained in molecular dynamics simulations of an expanding system with different initial excitation energies (temperatures) [3]. In Fig. 9 we have plotted the relative variance γ_2 versus the initial temperature (excitation energy) for different values of the total size of the system A_{tot} . One can see the signature of the critical point for the initial temperature $T = 5$ MeV where one exactly obtains a power law in the fragment size distribution. One also sees that the reduced variance diverges more and more sharply as A_{tot} increases. It is also interesting to compare the critical ratio $P_c / \rho_c T_c = M_0 / M_1|_{T_c}$, calculated at the point where one observes the peak for γ_2 , with other systems. For $A_{\text{tot}} = 100$ and $A_{\text{tot}} = 10^8$, one gets $M_0 / M_1 = 0.299$ and 0.298 , respectively. Our numerical simulation of the system in a box gives 0.317 , and Van der Waals equation gives 0.375 . Real gases give 0.287 for CO_2 , 0.290 for Xe and 0.305 for ^4He [10].

5. Conclusions

We have calculated by means of the virial theorem the equation of state of an infinite classical system in a cubic geometry with periodic boundary conditions and constant density. This equation of state has a critical temperature of 2.53 MeV and a critical density of 0.036 fm^{-3} , about $1/3$ the ground state density. We note that by using different numbers of particles in the box and different initialization and thermalization procedures, we obtain the same EOS with the same critical point. Another point is the decreasing of the critical temperature with the number of particles of the system. Several investigations of finite size effects on the critical temperature using Skyrme-type interactions [14] have concluded that the critical temperature goes down when decreasing the number of particles of the system. In our present work, it appears that this is not true and we have obtained for an infinite system (with periodic boundary conditions) the same critical temperature as the one observed in a previous work where we have studied, using the same two-body interaction the expansion of a finite system with 100 particles, passing during its evolution through the critical point. Furthermore, we have obtained at the critical point a fragment size distribution showing a power law with $\tau = 2.23$. The same power law was also observed for the expanding finite system for the critical evolution.

Finally, by making use of the grand partition function of the droplet model of Fisher, we have studied the critical behaviour of the moments of fragment size distributions and found the same behaviour as the one calculated by Campi. We have also extracted the equation of state of this model around the critical point shown that it is in good agreement with that calculated for the infinite classical system.

Acknowledgements

The authors acknowledge S. Ayik, M. Di Toro and V. N. Kondratyev for stimulating discussions. One of us (T.K.) thanks the theory group at INFN-LNS Catania for partial support and hospitality where the major part of this work was carried out.

References

- [1] J.E. Finn et al., Phys. Rev. Lett. 49 (1982) 1321; Phys. Lett. B 118 (1982) 458; H.H. Gutbrod, A.I. Warwick and H. Wieman, Nucl. Phys. A 387 (1982) 177c; M. Mahi, A.T. Bujak, D.D. Carmony, Y.H. Chung, L.J. Gutay, A.S. Hirsch, G.L. Paderewski, N.T. Porile, T.C. Sangster, R.P. Scharenberg and B.C. Stringfellow, Phys. Rev. Lett. 60 (1988) 1936; J.B. Elliot, M.L. Gilkes, J.A. Hauger, A.S. Hirsch, E. Hjort, N.T. Porile, R.P. Scharenberg, B.K. Srivastava, M.L. Tincknell and P.G. Warren, Phys. Rev. C 49 (1994) 3185; M.L. Gilkes et al., Phys. Rev. Lett. 73 (1994) 1590.
- [2] R. Balescu, Equilibrium and Nonequilibrium Statistical Mechanics (Krieger, Malabar, Florida, 1991).
- [3] V. Latora, M. Belkacem and A. Bonasera, Phys. Rev. Lett. 73 (1994) 1765; M. Belkacem, V. Latora and A. Bonasera, Phys. Rev. C 52 (1995) 271.

- [4] M.E. Fisher, Rep. Prog. Phys. 30 (1967) 615; Proc. International School of Physics, Enrico Fermi Course LI, Critical Phenomena, ed. M.S. Green (Academic Press, New York, 1971).
- [5] X. Campi, J. Phys. A 19 (1986) L917; Phys. Lett. B 208 (1988) 351; J. de Phys. 50 (1989) 183.
- [6] R.J. Lenk, T.J. Schlagel and V.R. Pandharipande, Phys. Rev. C 42 (1990) 372.
- [7] C.O. Dorso and J. Randrup, Phys. Lett. B 232 (1989) 29.
- [8] S. Pratt, C. Montoya and F. Ronning, Phys. Lett. B 349 (1995) 261.
- [9] S.E. Koonin and D.C. Meredith, Computational Physics (Addison Wesley, California, 1990).
- [10] K. Huang, Statistical Mechanics (John Wiley, New York, 1987).
- [11] A. Bonasera, F. Gulminelli and J. Molitoris, Phys. Reports 243 (1994) 1;
M. Belkacem, V. Latora and A. Bonasera, Phys. Lett. B 326 (1994) 21.
- [12] M.E. Fisher, Physics 3 (1967) 255.
- [13] J.E. Robinson, Phys. Rev. 83 (1951) 678.
- [14] H.R. Jaqaman, A.Z. Mekjian and L. Zamick, Phys. Rev. C 27 (1983) 2782; C 29 (1984) 2067.